Spatial localization of Langmuir waves generated from an electron beam propagating in an inhomogeneous plasma: Applications to the solar wind

A. Zaslavsky,[1] A. S. Volokitin,[2] V. V. Krasnoselskikh,[3] M. Maksimovic,[1] and S. D. Bale[4]

Received 21 October 2009; revised 19 January 2010; accepted 26 February 2010; published 26 August 2010.

[1] It is known from in situ observations that large-amplitude spatially localized Langmuir waves are frequent in the solar wind, and usually correlated with the presence of suprathermal electron beams, during type III events or close to the electron foreshock. It seems that the influence of the solar wind density fluctuations on the propagation effects of the Langmuir waves play an important role in the formation of these wave packets. In this article, we focus on the mechanism of generation of localized wave packets by electron beams propagating in an inhomogeneous medium. To this purpose, we present a theoretical model based on the resolution of the high-frequency component of the Zakharov's equation in which a source term describing the electron beam has been introduced, and show that this model is able to reproduce classical results about beam plasma instability and wave trapping in density cavities. Then we present simulation results of the generation of Langmuir wave packets in typical solar wind conditions at 1 A.U., and discuss the origin and nature of their localization.

Citation: Zaslavsky, A., A. S. Volokitin, V. V. Krasnoselskikh, M. Maksimovic, and S. D. Bale (2010), Spatial localization of Langmuir waves generated from an electron beam propagating in an inhomogeneous plasma: Applications to the solar wind, *J. Geophys. Res.*, *115*, A08103, doi:10.1029/2009JA014996.

1. Introduction

[2] The study of the beam-plasma interaction in specific solar wind conditions is a subject of great importance. It is well known that the propagation of an electron beam in an homogeneous plasma leads to the generation of Langmuir waves, that are electrostatic waves oscillating at the plasma frequency $\omega_p = (4\pi e^2 n_e/m_e)^{1/2}$, where n_e is the plasma electron density, e and m_e the electron charge and mass, respectively [*O'Neil et al.*, 1971; *Matsiborko et al.*, 1972].

[3] Among several known situations of beam-plasma interaction in the terrestrial neighborhood, the solar type III radio bursts are the most spectacular and studied examples of the propagation of energetic electrons in the coronal and interplanetary plasma. The scenario generally accepted for explaining these radio emissions is the following: energetic electrons are accelerated in the low corona during solar flares, and propagate in the antisunward direction exciting along their path Langmuir waves through beam-plasma instability. Then these electrostatic waves are partially converted into electromagnetic waves that are observed by earth based radio telescopes and spacecraft.

[4] Nevertheless, problems appear when quantitatively considering this scenario. Firstly, a simple linear calculation shows that for typical solar wind and beam parameters, the energetic electrons should be rapidly thermalized and not propagate to the observed distances (>1 A.U.) [*Sturrock*, 1964]. This problem is partially avoided considering the effect of the velocity dispersion of the beam: the waves generated by the particles at the head of the beam are reabsorbed by the particles arriving later, limiting the kinetic energy loss, as *Zaitsev et al.* [1972] showed it on analytical basis, assuming that the dynamics of the beam and the waves can be reproduced by the quasi-linear system of equations [*Vedenov*, 1967]. The question whether such equations are relevant to the modeling of type III solar bursts is still opened.

[5] The second point is related to the observed density fluctuations of the solar wind. Indeed, measurements by the ISEE spacecrafts [*Celnikier et al.*, 1983, 1987] or by scintillation observations [*Coles and Harmon*, 1978] show that density fluctuations (the amplitude of which can reach several percents of the solar wind density) are ubiquitous in the interplanetary medium. The study of the beam-plasma instability in the presence of such fluctuations shows that the diffusion of the waves by the density inhomogeneities should prevent any instability [*Nishikawa and Ryutov*, 1976], as the waves should be scattered out of the resonance with the beam on timescales smaller than the typical exponential wave growth time. As a consequence, no Langmuir waves, and then no radio signal should be observed at all.

[1]Observatoire de Paris, LESIA, Meudon, France.
[2]IZMIRAN, Troistsk, Russia.
[3]LPCEE, CNRS, Orleans, France.
[4]SSL, University of California, Berkeley, California, USA.

0148-0227/10/2009JA014996

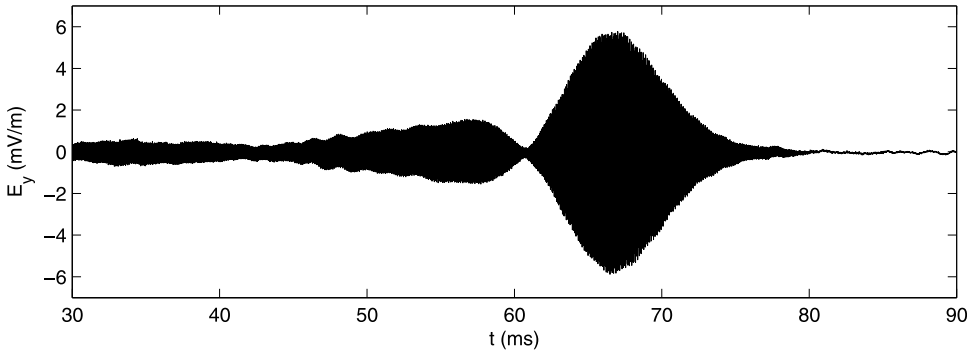

Figure 1. Example of localized Langmuir wave packets measured by the TDS instrument on board STEREO B, on 14 January 2007.

[6] To understand the observed wavefields, a theory of wave "stochastic growth" has been developed [*Robinson*, 1992; *Robinson et al.*, 1992], arguing that the waves can only grow in specific spatial regions called clumps, in which the geometry of the density fluctuations prevent the 3D diffusion of the waves out of the resonance with the beam (the direction of the density gradients should be in these regions aligned with the direction of the beam generating the waves, that is the direction of the magnetic field). In this case the waves growth rate evolution in time can be modeled as a random walk, and the distribution of the observed waves amplitudes should be lognormal as a consequence of the central limit theorem. This prediction fits well with the observations for small-amplitude waves [*Cairns and Robinson*, 1999], with some slight differences with log-normal distributions [*Krasnoselskikh et al.*, 2007], and reproduces the clumpy nature of the observed Langmuir Waves.

[7] Recent in situ observations by the TDS mode of the S/WAVES instrument equipping the STEREO spacecraft [*Bougeret et al.*, 2008] stimulated the theoretical investigation of these intense Langmuir waves (Figure 1 shows an example of a Langmuir waveform measured by the TDS instrument). The sampling time of this instrument is of 130 ms, allowing to capture a large number of full Langmuir waveforms, that happened to be spatially localized on scales of some hundreds of electron Debye lengths $\lambda_d = v_{the}/\omega_p$. Using these data, a study of the Langmuir wave decomposition process into an ion sound wave and a daughter Langmuir wave have been realized [*Henri et al.*, 2009], and a procedure to determine the solar wind plasma density fluctuations at small scales has been developed [*Kellogg et al.*, 2009]. In the present work, we interest ourselves in the formation of these localized wave packets. *Ergun et al.* [2008] proposed that propagation effects of Langmuir waves in the inhomogeneous solar wind plasma were at the basis of the observed spatial localization, and showed, using the high-frequency component of Zakharov's equations [*Zakharov*, 1972] as a propagation equation for the Langmuir waves, that several waveforms could be interpreted as trapped eigenmodes of parabolic density cavities.

[8] The purpose of this paper is to present a model of wave-particle interaction based on the spectral resolution of the high-frequency component of Zakharov's equations in which a term relative to beam particles has been added. As exposed in the following, our approach enables to reproduce the eigenmode structure of the electric field in the presence of density fluctuations, and to study the interaction of this field with a beam of charged particles.

[9] For reasons of simplicity and of numerical simulations durations, we shall limit ourselves to the 1D case. This can be justified by the observed wavefields that are mainly linearly polarized along the magnetic field direction [*Ergun et al.*, 2008], and by the fact that as previously mentioned, the wave growth is supposed to occur in clumps in which the density gradients are aligned with the direction of propagation of the beam, so that a 1D modeling of the wave growth in such clumps seems reasonable.

[10] Let us finally note that the phenomenon that we study in this work is related to nonlinear propagation effects of the Langmuir waves, and is of a fundamentally different nature to the self-focusing of Langmuir waves, in which the ponderomotive force exerted by the localized electrostatic field on the quasi-neutral plasma plays a crucial role. We shall here consider that the electrostatic energy of the waves is always sufficiently small compared to the electron thermal energy for the effect of the ponderomotive force to be neglected, and do not consider the low-frequency Zakharov's equation in the present model.

[11] In section 2, we present the analytical model that we developed and which is numerically solved in the presented simulations. Sections 3 and 4 are devoted to the validation of this model: we expose results of numerical simulations of classical plasma physics results (beam plasma instability in an homogeneous plasma and Langmuir wave trapping in a density cavity in sections 3 and 4, respectively) and show that the numerical code provides results in quantitative agreement with the plasma physics theory. Section 5 presents the results of beam-plasma interaction in the presence of gaussian and turbulent density profiles. Section 6 summarizes the main results and concludes the article.

2. Presentation of the Model

[12] The model that we present is designed for the description of the beam-plasma interaction in a slightly inhomogeneous plasma. In the solar wind, density fluctuations $\delta n/n$ of typical amplitude of ~1% are ubiquitous. They are thought to be generated by the solar wind fluid or MHD turbulence. Here we are not interested by their origin or stability, and shall just consider them through a given function $\delta n(x, t)$ of space and time. In this case, the propa-

gation of the Langmuir waves is described by the high-frequency component of the Zakharov's equations [*Zakharov*, 1972], and their interaction with resonant particles can be accurately treated using a spectral method that we expose in this section.

[13] In our treatment, we neglect the electrostatic potential associated with the plasma density inhomogeneities. This potential is of the order of $e\phi/k_bT_e \sim \delta n/n \sim 10^{-2}$, that is much smaller than the potential of the Langmuir waves considered in this article. Moreover, this potential does not influence the dynamics of the electron beam, since it is not resonant with it (the resonant velocity associated with the density inhomogeneity is the ion sound velocity $c_s \sim (m_e/m_i)^{1/2}v_{the}$, which is much smaller than the considered electron beam velocities).

[14] Let us finally note that the use of this method has already given results in the frame of the study of the interaction between resonant particles and oblique waves in homogeneous magnetized plasmas [*Volokitin and Krafft*, 2004; *Zaslavsky et al.*, 2006].

2.1. Set of Equations

[15] To describe the interaction of resonant electrons with waves propagating in a plasma with given density fluctuations $\delta n(x, t)$, we derive the high-frequency component of the Zakharov's equations adding an external charge density $-en_b(x, t)$ as a source term in Poisson equation (n_b is the density of the electron beam):

$$\nabla\left(i\frac{\partial}{\partial t}E+\frac{3\omega_p}{2}\lambda_d^2\frac{\partial^2}{\partial x^2}E-\omega_p\frac{\delta n}{2n_0}E\right)=-2\pi en_b(x,t)\omega_p e^{i\omega_p t} \tag{1}$$

In this equation $E(x, t)$ is the electric field envelope, the actual electric field undergone by the particles being equal to $\Re(E(x, t)e^{-i\omega pt})$. We take the Fourier transform in space of this equation, using the conventions (for any function $F(x, t)$ of space period L),

$$F(x,t)=\sum F_k(t)e^{ikx}, \tag{2}$$

the Fourier component being

$$F_k(t)=\int_0^L F(x,t)e^{-ikx}\frac{dx}{L}, \tag{3}$$

and we describe the beam through N macroparticles using the discrete density function (introducing the spatially averaged beam density $\overline{n_b}$),

$$n_b(x,t)=\frac{\overline{n_b}L}{N}\sum_\alpha \delta(x-x_\alpha(t)), \tag{4}$$

so that

$$n_{bk}=\frac{\overline{n_b}}{N}\sum_\alpha e^{-ikx_\alpha(t)}. \tag{5}$$

[16] One then obtains the evolution equation for the Fourier component of the slowly varying envelope $E_k(t)$ in the form

$$\left(\frac{d}{dt}+i\Omega_k\right)E_k=-i\frac{\omega_p}{2n_0}(\delta nE)_k+p_k\sum e^{-i\left(kx_\alpha-\omega_p t\right)} \tag{6}$$

where the following notations have been introduced for reasons of clarity: $\Omega_k=\frac{3}{2}\omega_p\lambda_d^2k^2$ and $p_k=2\pi e(\overline{n_b}/N)(\omega_p/k)$.

[17] The system is closed by the equations for the dynamics of the N macroparticles composing the beam

$$d_t x_\alpha=v_\alpha,\qquad d_t v_\alpha=-\frac{e}{m}\Re\sum E_k e^{i\left(kx_\alpha-\omega_p t\right)}, \tag{7}$$

for $\alpha = 1, \ldots, N$. One can check that this system of equations preserves the total energy

$$E=\sum_\alpha\left(\frac{1}{2}mv_\alpha^2-e\Re\sum_k(iE_k/k)e^{i\left(kx_\alpha-\omega_p t\right)}\right)+\sum_k\left(\omega_p+\Omega_k\right)\frac{E_k^*E_k}{2kp_k} \tag{8}$$

as well as the generalized impulse

$$P=\sum_\alpha mv_\alpha+\sum_k\frac{E_k^*E_k}{2p_k}. \tag{9}$$

[18] Despite this property will not be used in the frame of this article, let us finally note that the equations (6) and (7) have an Hamiltonian structure (a textbook dedicated to such Hamiltonian models of wave particle interactions in plasmas has been published by *Elskens and Escande* [2003]), that can be useful to perform analytical perturbation calculation, and to build symplectic numerical schemes [*Sanz-Serna and Calvo*, 1994].

2.2. Numerical Method

[19] A numerical code integrating the system of equations (6) and (7) has been developed, using a classical leapfrog numerical scheme in which the nonlinear term $\propto (\delta nE)_k$ is evaluated at each time step using a Fast Fourier Transform algorithm. To check the validity of our numerical scheme, the quantities (8) and (9) have been monitored in all the numerical simulations performed, and we adapted the time step so that their relative variations always stay below one percent.

[20] All the results presented in this article are obtained using a spectral grid composed of 512 points periodically distributed in Fourier space between $-k_{\max}$ and $k_{\max}$, and a periodic box of spatial dimension $L = 4000\lambda_d$, so that $\lambda_d\Delta k_{grid} = 0.0016$ and $\lambda_d k_{\max} = 0.4$. The results presented in Figures 1–9 are normalized with quantities λ_d for lengths, ω_p^{-1} for times (i.e., the velocities are normalized by the electron thermal velocity $v_{th} = \omega_p\lambda_d$), m for masses and e for electric charges.

3. Dispersion Relation Neglecting the Density Fluctuations

[21] In this section, we look for the dispersion relation of the Langmuir waves in the presence of an electron beam, when the amplitudes of the electric field and the density fluctuations are small enough to neglect the nonlinear term in (1), or more simply when no density fluctuations are

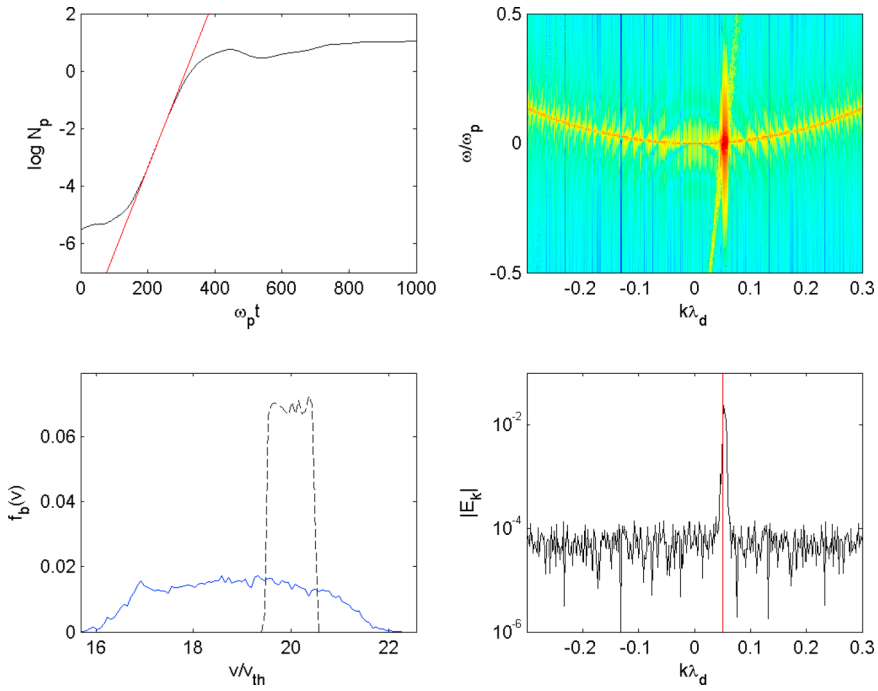

Figure 2. Interaction between a cold electron beam and a plasma with no density fluctuations. The main parameters are $N = 16384$, $v_b/v_{th} = 20$, and $n_b/n_0 = 4 \cdot 10^{-5}$. (top left) The logarithm of the number of plasmons as a function of time. The observed growth rate is $\gamma \sim 0.03\omega_p$ (overplotted slope). (top right) The logarithm of the space-time Fourier transform of the electric field envelope (arbitrary units), in which the two branches of the dispersion relation (13) are visible. (bottom right) The destabilized wave spectrum at the final time of the simulation, on which the resonant wave vector $k = \omega_p/v_b$ has been overplotted. (bottom left) The initial (dashed) and final (solid) electron velocity distribution function.

present in the plasma. To fulfill this goal, we linearize equations (6) and (7) using the conventions

$$x_\alpha = x_{\alpha 0} + v_\alpha t + \delta x_\alpha, \qquad E_k = 0 + \delta E_k.$$

We obtain

$$\frac{d^2}{dt^2}\delta x_\alpha = -\frac{e}{m}\Re \sum_k \delta E_k e^{i\left[kx_{\alpha 0} + \left(kv_\alpha - \omega_p\right)t\right]} \tag{10}$$

$$\frac{d}{dt}\delta E_k = -i\Omega_k \delta E_k + p_k \sum_\alpha -ik\delta x_\alpha e^{-i\left[kx_{\alpha 0} + \left(kv_\alpha - \omega_p\right)t\right]} \tag{11}$$

Looking for a solution of this linearized system under the form $\delta E_k = E_{k0}e^{-i\Omega t}$, one obtains for Ω the dispersion relation

$$\Omega = \Omega_k + \omega_p \frac{\overline{n_b}}{2n_0}\frac{1}{N}\sum_\alpha \frac{\omega_p^2}{\left(kv_\alpha - \omega_p - \Omega\right)^2} \tag{12}$$

In the case that we shall consider in this article, in which we can neglect the velocity spreading of the beam ($\Delta v_b/v_b \ll 1$), we have $v_\alpha \sim v_b$ for all α, and

$$\left(\Omega - \Omega_k\right)\left(\Omega + \omega_p - kv_b\right)^2 = \omega_p^3(\overline{n_b}/2n_0). \tag{13}$$

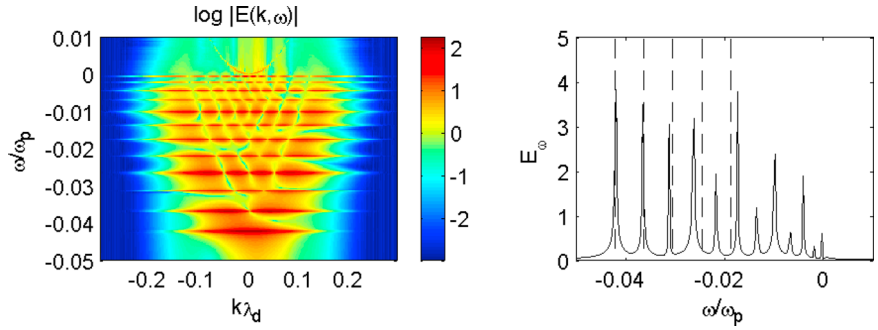

Figure 3. Excitation of the eigenmodes of a gaussian density cavity. The main parameters are $\delta n_{\max}/n_0 = -0.09$ and $\sigma_{\delta n} = 63\lambda_d$. (left) The logarithm of the space-time Fourier transform of the electric field envelope, exhibiting the discrete structure of the trapped waves field. (right) The time Fourier transform of the envelope (arbitrary units), on which analytical predictions (16) have been overplotted for the eigenfrequencies corresponding to $n = 0, \ldots, 4$.

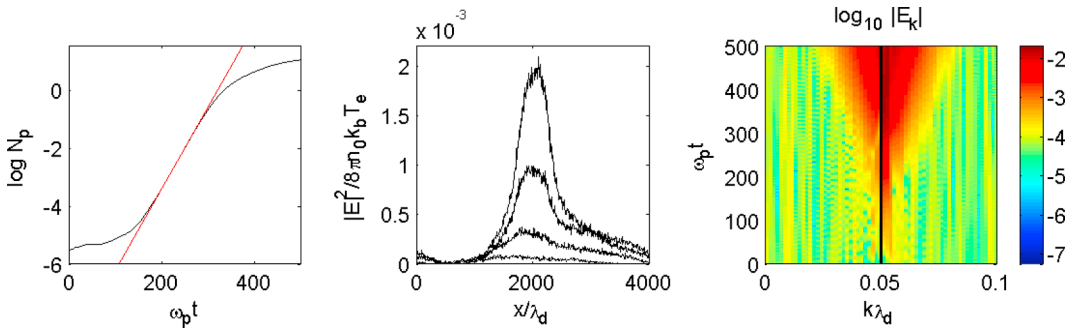

Figure 4. Linear stage of a beam plasma instability (same beam parameters as in Figure 2) in the presence of a gaussian density cavity characterized by $\delta n_{\max}/n_0 = -0.03$ and $\sigma_{\delta_n} = 200\lambda_d$. (left) The logarithm of the number of plasmons as a function of time. The straight line is a linear fit with a slope $\gamma = 0.03\omega_p$. (middle) The electrostatic energy density profile at four different times ($\omega_p t = 250$, 300, 350, and 400 from bottom to top) at the end of the linear phase. (right) The evolution in time of the wave spectrum (logarithmic scale) during the linear stage, on which the resonant wave vector $k = \omega_p/v_b$ is overplotted.

This dispersion relation exhibits two resonant branches: one corresponds to $\Omega_L \sim \Omega_k$, and corresponds to Langmuir waves; the second is $\Omega_B \sim kv_b - \omega_p$ and corresponds to beam modes. In the usual case where $v_{th} \ll v_b$ (i.e., $k\lambda_d \ll 1$), the solution of (13) is

$$\frac{\Omega}{\omega_p} \simeq \left(\frac{\overline{n_b}}{2n_0}\right)^{1/3}\left(-\frac{1}{2} + i\frac{\sqrt{3}}{2}\right) \tag{14}$$

where we retained the solution with positive imaginary part, that is, the unstable mode. The formula (14) is the classical result on cold beam instability, that can be found in most of plasma textbooks. Figure 2 shows the result of the numerical simulation of the beam plasma instability in the hydrodynamic regime $\Delta v_b/v_b \ll 1$. The beam distribution is taken to be initially homogeneous in a region of phase space $[0, L] \times [v_b - \Delta v_b/2, v_b + \Delta v_b/2]$, with $v_b = 20v_{th}$ and $\Delta v_b/v_b = 0.05$. The results illustrates the dispersion relation (13), showing that our numerical code provides results in good agreement with the classical plasma theory. The number of plasmons shown in Figure 2 characterizes the intensity of the electric field, and is defined by $N_p(t) = \int W(x, t).dx$, where $W(x, t) = |E(x, t|^2/8\pi n_0 k_B T_e$ is the normalized electrostatic energy density. For the case of an hydrodynamical instability where the destabilized wave spectrum is very narrow, N_p should grow with a growth rate $\gamma = \sqrt{3}(n_b/2n_0)^{1/3}\omega_p$, which is of the order of the one observed in the simulation; nevertheless, the width of the initial distribution function is not negligible, so that the observed growth rate is smaller than the estimate (14), which is the maximum growth rate occurring for a totally monokinetic electron beam. The

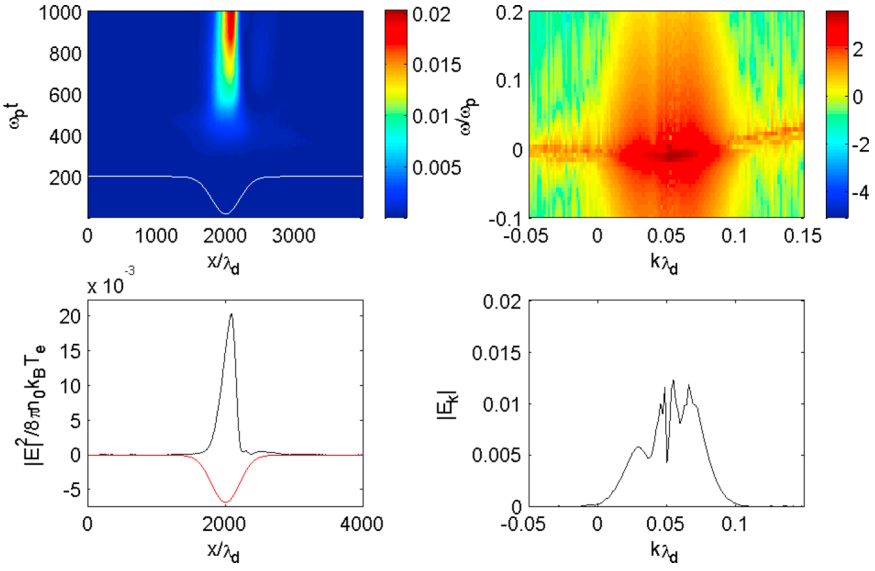

Figure 5. (top left) Langmuir waves normalized electrostatic energy $W(x, t)/n_0 k_B T_e$ as a function of space and time and (top right) logarithm of the space-time Fourier transform of the electric field envelope as a result of a beam plasma instability (same beam parameters as in Figure 2). (bottom left) Cut of $W(x, t)/n_0 k_B T_e$ at $\omega_p t = 1000$ and (bottom right) space Fourier transform of the electric field at the same time. The density profile is overplotted (arbitrary units) in Figure 5 (left).

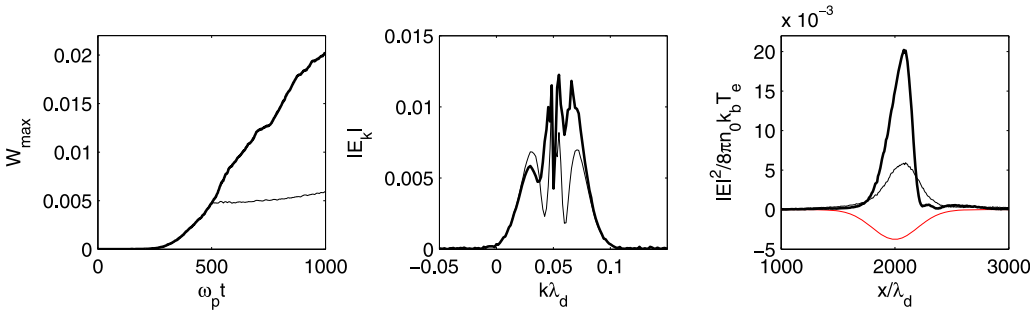

Figure 6. Thick line, simulation with resonant particles; thin line, without resonant particles (propagation effects only). (left) Maximum of the normalized wave energy density $W(x, t)$ as a function of time, showing clearly the enhancement of energy in the density cavity due to the nonlinear wave-particle effects. (middle) The k spectra at $\omega_p t = 1000$. (right) Normalized wave energy density $W(x)$ at $\omega_p t = 1000$.

evolution of the electron velocity distribution function is also the one expected: the particle distribution diffused in velocity space to a state of smaller average velocity.

4. Trapped Eigenmodes in Absence of Beam Particles

[22] To ensure that our model accurately reproduces the structure of the Langmuir wavefield in the presence of density inhomogeneities, and in particular that it is able to reproduce the eigenmode structure of the trapped waves, we performed a simulation of the evolution of a spatially narrow wavefield (in order to excite a k spectrum as broad as possible) trapped in a gaussian density cavity, described by

$$\delta n = -\delta n_{\max} e^{\frac{(x-L/2)^2}{2\sigma_{\delta n}^2}}, \qquad (15)$$

in the absence of any particle beam. The results are displayed in Figure 3, and show the discrete structure of the trapped waves (i.e., with $\Omega < 0$) coexisting with freely propagating Langmuir waves at $\Omega \sim \Omega_k$ (continuous eigenmodes). The form of the eigenfunctions is complicated to obtain for a gaussian density cavity (approximate eigenvalues are calculated by *Stephenson* [1977]), but one can easily find the analytical form of the first trapped modes using a Taylor expansion of the density profile near its minimum: $\delta n \simeq -\delta n_{\max}(1 - x^2/2\sigma_{\delta n}^2)$. The problem then reduces to the one of a parabolic density cavity, for which exact solutions of the Zakharov's equation (1) can be found, as done by *Ergun et al.* [2008], under the form of a linear combination of the discrete eigenmodes $E_n = A_n(x)e^{-i\Delta\omega_n t}$, where the eigenfrequencies are given by

$$\Delta\omega_n/\omega_p = -\frac{\delta n_{\max}}{2n_0} + \left(n + \frac{1}{2}\right)\sqrt{\frac{3\delta n_{\max}}{2n_0}}\frac{\lambda_d}{\sigma_{\delta n}} \qquad (16)$$

and the spatial waveforms (eigenfunctions) are

$$A_n(x) \propto H_n(Qx)e^{-Q^2x^2/2}, \qquad Q^2 = \frac{\sqrt{\delta n_{\max}/6n_0}}{\lambda_d\sigma_{\delta n}}. \qquad (17)$$

Here H_n is the n^{th} Hermite polynomial. Figure 3 shows that our simulation results are in very good agreement with the theoretical predictions (16) and (17) for the most deeply trapped eigenmodes ($n = 0,1,2$), and that this agreement is, as expected, less good for higher harmonics, for which the difference between the gaussian shape of the density hole and its parabolic approximation has to be taken into account. Let us note that the parameter describing the density cavity are exaggerated in this simulation ($\delta n_{\max}/n_0 \sim 10\%$, $\sigma_{\delta n} \sim 60\lambda_d$) in order to obtain a field structure as visible and clear as possible.

5. Simulation of the Beam-Plasma Instability in Presence of Density Inhomogeneities

[23] In this section, we present results of numerical simulations of the interaction of an electron beam with various density profiles. It is important to note that the simulations are performed in a regime in which the propagation term $\propto (\partial^2/\partial x^2)E$ is smaller than the term $\propto \delta nE$ describing the effect of plasmon diffusion on the density gradients in equation (1). This case has in our knowledge never been investigated, whereas it should be relevant to the solar wind in which relative density fluctuations of the order of the percent are observed. We show that in this regime, after a stage of linear instability similar to the one appearing in an homoge-

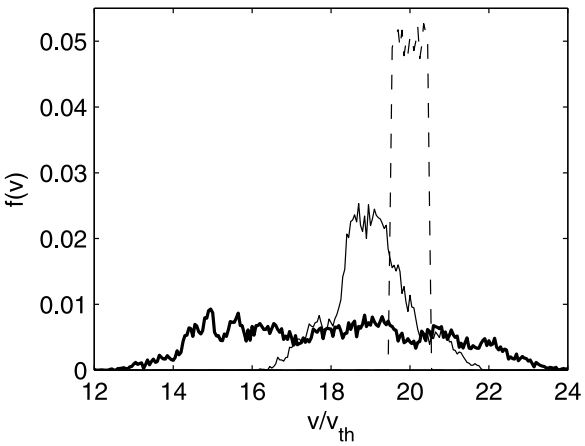

Figure 7. Electron velocity distribution function evolution during the beam plasma instability in the presence of a gaussian density cavity. Dashed line, $\omega_p t = 0$; thin line, $\omega_p t = 500$; thick line, $\omega_p t = 1000$.

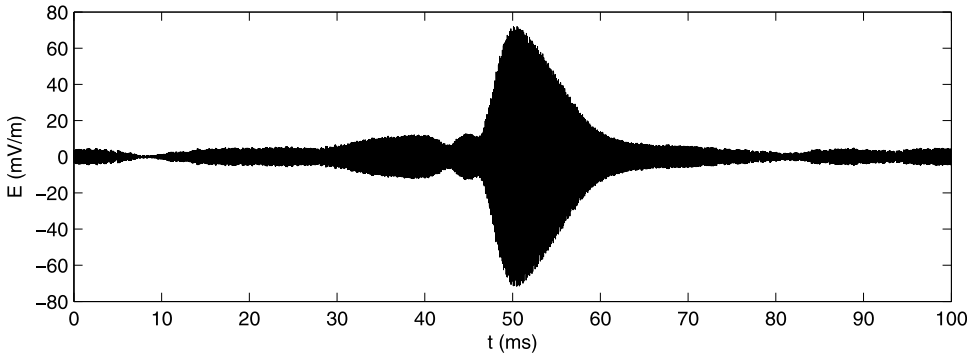

Figure 8. Electric waveform that would observe a spacecraft initially located at $x/\lambda_d = 4000$ assuming that the electric field envelope is frozen in the state reached at the end of the simulation ($\omega_p t = 1000$) during the observation. The solar wind parameters used are described in the beginning of section 5.1, and the advection speed of the solar wind is taken to be $V_{SW} = 300$ km/s.

neous plasma, the nonlinear effects tend to focalize the electric field energy in the density cavities of the plasma.

[24] First of all, let us note that we shall consider here only time-independent density profiles, to make as clear as possible the physical interpretation of the simulations results. The time durations τ_{sim} of the simulations are taken to be of roughly $1000\omega_p^{-1}$. Assuming that the density fluctuations considered here are ion sound waves, their typical evolution time is $\tau_{\delta n} \sim \sigma_{\delta n}/c_s$, where $c_s^2 = k_B T_e/m_i$ is the ion sound velocity (here we neglect the ion temperature effect), that is $\tau_{\delta n} \sim (m_i/m_e)^{1/2}\sigma_{\delta n}/v_{th}$. For the examples considered here, one has $\tau_{\delta n} \sim 8000\omega_p^{-1}$, so that we can neglect the time evolution of the density fluctuations on the simulated timescales.

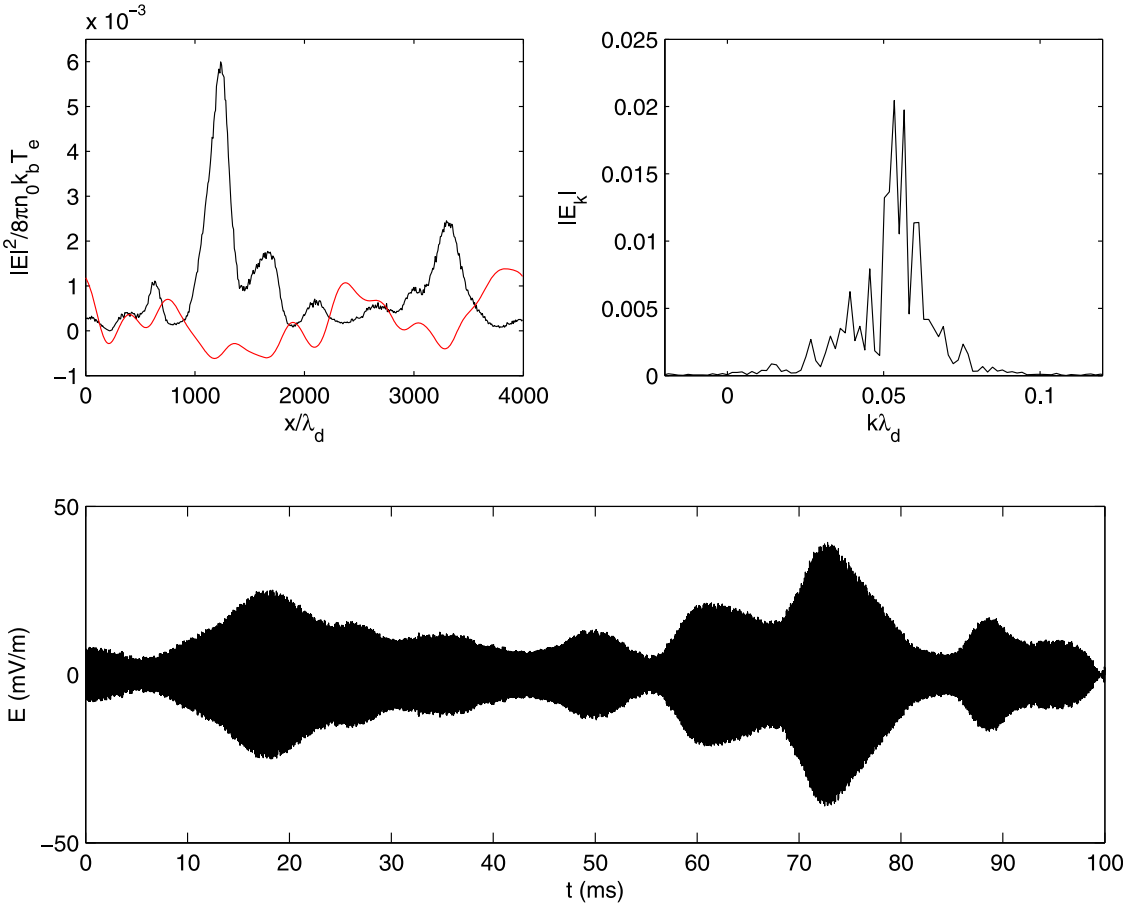

Figure 9. (top left) Normalized electrostatic energy density as a function of space at $\omega_p t = 1000$, after a beam plasma instability with the same beam parameters as Figure 2. The red line shows the turbulent density profile (arbitrary units). (top right) Electric field k spectrum at $\omega_p t = 1000$. (bottom) The waveform reproduced using the same method as for Figure 8.

[25] Another important point is that the thermal Landau damping has been neglected in equation (1). The timescale on which the damping of the Langmuir waves occurs is the inverse of the damping rate $\gamma_L \simeq (\pi\omega_p^3/2k^2)\partial_v f_e(v = \omega_p/k)$, so that for a Maxwellian plasma and for waves in resonance with the beam, one has $\gamma_L \sim 10^{-80}\omega_p$ and can clearly be neglected in our simulations. Anyway for simulation times of a thousand plasma period, the damping should be taken into account for waves with $k\lambda_d > 0.2$, and it is checked in all our simulations that no signal is present for such wave vectors.

5.1. Choice of the Initial Conditions

[26] We perform simulations in a range of parameters relevant to the solar type III electron beams observed at 1 A.U. We take for the solar wind parameters the following typical values at 1 A.U.: $T_e \sim 10^5$ K and $n_0 \sim 5.10^6$ m^{-3}, so that $\lambda_d \sim 10$ m, $f_p = \omega_p/2\pi \sim 20$ kHz, and $v_{the} \sim 10^6$ m/s.

[27] Concerning the impulsive electrons, they are launched at a velocity $v_b = 20v_{the}$, that is $v_b \sim c/10$ which corresponds to an average velocity of the type III exciters (that ranges usually from $c/20$ to $c/3$). The observed velocity dispersion of the beams is quite small and is taken in our simulations to be $\Delta v_b/v_b = 0.05$. All these parameters are consistent with the measurements performed by the Wind spacecraft [*Ergun et al.*, 1998] of a type III burst observed on 5 April 1995. An important parameter characterizing the beam is its density. The ratio n_b/n_0 has been taken around 10^{-5} in order to obtain a good signal-to-noise ratio in our numerical simulations, and to obtain a growth rate large enough to observe the instability and its saturation during the $1000\omega_p^{-1}$ time of simulation. We must note that this growth rate is clearly over estimated compared to the observations. Nevertheless, as detailed below, this choice does not affect the main physics of the wave focusing effect discussed in this article. As this parameter also determines the electrostatic energy density of the Langmuir waves at the saturation of the beam instability ($W \propto (n_b/n_0)^{4/3}$), the electric field intensities obtained in our simulations will be higher than the one observed by the TDS instrument on S/WAVES.

[28] The simulation box with periodic boundary conditions is taken with a length $L = 4000\lambda_d$, which enables to study gaussian density holes in the range of width $\sigma_{\delta n} = 20$–$500\lambda_d$. In the following we shall focus on the typical case of a density hole characterized by $\sigma_{\delta n} = 200\lambda_d$ and $\delta n_{\max}/n_0 = -0.03$.

5.2. Linear Stage of the Instability

[29] Figure 4 shows the number of plasmons, that is $N_p(t) = \int W(x, t).dx$ as a function of time, and the time evolution of the wave spectrum in k space until the saturation of the instability, which we roughly defined to happen when the $N_p(t)$ function stops to grow exponentially, that is at $\omega_p t \sim 500$. We can see that the instability is comparable to the case in which no density fluctuations is present (see Figure 2): the plasmon number increases with an exponential growth rate $\gamma/\omega_p \sim 0.03$, and the wave spectrum is mainly monochromatic and peaked around the most unstable mode $k = \omega_p/v_b$. Nevertheless, one can clearly see the influence of the density perturbation through the broadening of the k spectrum that appears after $\omega_p t \sim 250$, and to the corresponding enhancement of the electrostatic energy close to the minimum of the density profile.

[30] These results can be understood with the help of equation (6) for the most unstable mode. The order of magnitude of the terms composing the evolution equation for E_k are: $\Omega_k/\omega_p = (3/2)k^2\lambda_d^2 \sim (v_{the}/v_b)^2 \sim 1/400$ for the linear propagation term whereas it is of $\delta_n/2n_0 \sim 1/70$ for the "focusing" term and $\gamma_k/\omega_p \sim (n_b/n_0)^{1/3} \sim 1/30$ for the wave-particle interaction term. Thus during the linear stage of the instability the linear propagation effects can totally be neglected. The two dominant effects are the exponential wave growth, which is homogeneous in space, and the focusing effects that start to play a role after a few e-folding of the electric field.

[31] This order of magnitude hierarchy is changed when considering the actual beam plasma instability at 1 A.U., as the observations suggest much smaller growth rates. In this case the wave-particle term γ_k/ω_p would become the smallest one, the two others terms being unchanged. Thus, the dominant effect during the linear stage would be the broadening of the wave spectrum responsible for the wave localization discussed in section 5.3. As this effect does not depend on the amplitude of the electric field (the high-frequency Zakharov's equation being linear with respect to $E(x, t)$), but rather on the shape of the density fluctuation $\delta n(x)$, the localization of the waves would not be changed in its nature, but would happen simultaneously with the electric field exponential growth.

5.3. Nonlinear Stage of the Instability

[32] Figure 5 shows the normalized electrostatic energy density $W(x, t)/n_0 k_B T_e$ as a function of space and time as a result of a beam-plasma instability in the presence of a gaussian density cavity: after the linear stage of the instability, in which the wave growth is quite homogeneous in space, the electrostatic energy generated from the beam is strongly focalized inside the density cavity.

[33] The Fourier transform of the electric field envelope shown in Figure 5 shows that no energy is present in the negative wave vectors, meaning that no plasma wave reflection had time to be realized at $\omega_p t = 1000$. In this case it is clear that no trapped eigenmode is present in the density cavity. Nevertheless, a spatial localization of the electrostatic energy in the density cavity is clearly visible, that can be understood as follows. During the initial stage of the simulation, the beam is nearly monokinetic, so that it generates an essentially monochromatic wave spectrum, peaked at the resonant wave vector $k_{res} = \omega_p/v_b$. The electrostatic energy deposition from the beam is thus homogeneous in space. Then the nonlinear focusing effect starts to play a role and the wave spectrum is broadened by the resonant coupling between the Langmuir waves and the density perturbation. This process is described by the term

$$(\delta nE)_k = \sum_{k'+k''=k} \delta n_{k'} E_{k''} \tag{18}$$

so that starting from the monochromatic resonant Langmuir wave, the wave spectrum evolution is given by

$$\left(\frac{d}{dt} + i\Omega_k\right) E_k \sim -i\frac{\omega_p}{2n_0} E_{k_{res}}(t=0)\delta n_{k-k_{res}} \tag{19}$$

where $\delta n_{k-k_{res}} \propto \exp - \pi^2\sigma_{\delta n}^2(k - k_{res})^2$. Then the initial evolution of the wave spectrum consists in a gaussian broadening, that can be seen in Figure 4 (right) and Figure 5 (right). In real space, a gaussian bump thus develops in the wave energy profile, spatially correlated with the density cavity. After this initial gaussian broadening, the evolution due to the coupling term (18) is more complicated to describe mathematically; nevertheless it is clear that it will act to broaden the spectrum until reflection of the waves occurs (the simulation is stopped just before the reflection of the first plasmons).

[34] It can be seen in real space that the maximum of the energy density is not located at the minimum of the density profile, but in the positive density gradient region located at the right of the minimum, that is the location of the reflection points of the waves destabilized inside the hole (and which thus oscillate at a frequency slightly below the average plasma frequency).

[35] Thus, the propagation effects of the Langmuir waves in the inhomogeneous plasma explains the spatial localization of the waves in the density cavities. In addition, our models enables to investigate the combined effects of the resonant particles on this focusing. To distinguish between both, we performed a simulation without any beam particles (that is, setting the right-hand term of (1) to zero), taking as initial condition the electric field at the saturation of the instability in the case discussed in the previous pictures (that we defined to be $\omega_p t = 500$), and letting it evolve until $\omega_p t = 1000$.

[36] The results of this simulation are presented in Figure 6, and show that the electrostatic energy localized in the hole is more important in the presence of resonant particles. We shall not quantitatively investigate this phenomenon in this article, nevertheless, we can qualitatively understand it through the following considerations. In the absence of resonant particles, the nonlinear propagation effects tend to focalize the energy already present in the hole at the reflection points. Then there is an increase of the maximum of the energy density $W_{\max}$ with time, but no increase of the total energy present in the hole, as the equation (1) preserves the total number of plasmons when its right hand term is set to zero. The picture is different in the presence of resonant particle: the focusing of the electric field that occurred during the linear stage of the instability influences the motion of the particles, that becomes chaotic (as the resonant domains of different waves are overlapping [see *Chirikov*, 1979]). This motion, and the consequent diffusion of the electron velocity distribution function results, as illustrated in Figure 6, in an energy transfer from the particles to the waves, and in particular in a enhancement of the wave energy spatially localized in the density hole. The effect of the resonant particles can be understood in more details looking at the k spectra at the end of both simulation: when resonant particles are present, the distribution of $|E_k|$ is not symmetric anymore: particles have taken energy from the small k waves (that is, the one that have high phase velocities and thus accelerates the beam particles) and have given energy to the high k waves, that are the one decelerating particles in average. This can be seen on the particle distribution function shown in Figure 7: a large diffusion has happened between the saturation stage and the end of the simulation. Comparing this distribution with the one shown in Figure 2, we can see that the diffusion is more efficient when a density cavity is present ($v_{\min} - v_{\max} = 14$–24) than in the case of an homogeneous plasma ($v_{\min} - v_{\max} = 16$–22).

[37] The case of charged particle diffusion by a gaussian wave packet is treated by *Fuchs et al.* [1985], but the consistent effect of this diffusion on the wave evolution has (to our knowledge) never been studied. The equations treating this subject should generalize the quasi-linear equations with no averaging on the waves phases as this information is essential to describe the spatial localization of the total field energy.

[38] Finally to enable a comparison of our results with the waveforms captured by the instruments on board the WIND or STEREO spacecraft, we show in Figure 8 the waveform that would observe a spacecraft assuming that the electric field is frozen in the state reached at the end of the simulation. This is shown only for example, firstly because the beam density is overestimated, giving electric field amplitudes too high by a factor of two compared to the most intense Langmuir Waves observed, and secondly because the "frozen field" assumption actually does not hold on physical basis: the time for the considered solar wind portion to pass by the spacecraft location is $T = L/V_{SW} \sim 100$ ms $\sim 10000\omega_p^{-1}$ that is much larger than our simulation times, and should be larger than the typical time of stability of the considered density structures. This last point raises the matter whether the reproduction of the waveforms measured by an instrument like TDS can be done on the basis of a time-independent model (in which the fields are considered as constant in time during the 100 ms time of the measurement).

5.4. Case of a Turbulent Density Profile

[39] We previously considered the case of a gaussian density cavity in order to obtain a clearly understandable physical picture. Now we investigate the more realistic case of a random density profile, with valleys and hills having an amplitude of 1% of the solar wind density, and with typical wave vectors comparable with the resonant Langmuir wave vector ω_p/v_b so that wave trapping can occur. Figure 9 summarizes the result of a simulation of beam-plasma interaction with parameters similar to the previous simulations, but with a random density profile. The latter was obtained by taking a gaussian power spectrum for the density $\delta n_k \propto \exp(-k^2/\sigma_k^2)$ with $(\lambda_d\sigma_k) = 10^{-2}$, and by multiplying each Fourier component by $\exp(i\theta)$ with θ taken randomly in the interval $[0, 2\pi]$. We then compute the real part of the inverse Fourier transform to obtain the density profile in real space.

[40] One clearly sees that at the end of the simulation time $t \sim 1000\omega_p^{-1}$, the electrostatic energy profile is anticorrelated with the density profile: large-amplitude localized wave packets have formed close to the local density minima whereas the electrostatic energy almost vanishes in the overdense regions. As in the previously presented simulations, no wave signal is present in the negative wave vectors, and thus no eigenmode structures have been formed: we observe a spatial localization of the electric field due to the

broadening of the destabilized wave spectrum through propagation and nonlinear wave-particle interaction.

6. Conclusions and Perspectives

[41] In this article, we presented an original tool to study the self consistent interaction between plasma waves and a resonant beam of particle in a slightly inhomogeneous medium, based on the spectral resolution of the high-frequency component of the Zakharov's equations in which a term relative to the dynamics of the beam particles had been added. We first showed, in sections 2 and 3, that the developed model and the associated numerical code were able to recover the classical results about the cold beam instability in an homogeneous plasma and about the Langmuir wave trapping in density cavities.

[42] Then we used the numerical code to investigate the destabilization of electrostatic waves by a beam of suprathermal particles in an inhomogeneous plasma, this topic being of central interest for the understanding of the Langmuir waveforms in situ observations by spacecrafts exploring the solar wind, especially during type III bursts events.

[43] The main results is that on the typical timescale of stability of the considered density holes, the discrete eigenmode structure of the trapped waves does not have time to be established. Instead, we observe a broadening of the wave spectrum, resulting in a spatial localization of the Langmuir wavefield correlated with the density cavities. More precisely, the maximum of the electrostatic energy is located in the positive gradient regions located after the local minima of the plasma density, which is coherent with the solution of the WKB equations for Langmuir waves propagation, despite we are not in the domain of validity of this equation for the considered density gradients as the destabilized wave vectors do not check the WKB assumption that can be written in our case $k\sigma_{\delta n} \gg 1$. Moreover, we showed that this spatial localization of the Langmuir waves in the density cavities is enhanced by the nonlinear interaction between the resonant particles and the waves. This effect has only been qualitatively studied and should be more quantitatively investigated in the future.

[44] Let us finally recall that the results presented are obtained in a regime in which the Langmuir waves growth rate is much higher than the one evaluated from in situ observations realized during solar type III bursts events. This choice has been done for the instability to develop on a $\sim 1000\omega_p^{-1}$ timescale, so that the numerical simulation could be performed in a reasonable computational time. The choice of the $1000\omega_p^{-1}$ simulation duration was also done as it was identified as the timescale on which we could consider the density inhomogeneities to be time independent. In the more realistic regime where $\gamma/\omega_p \ll k^2\lambda_d^2 \ll \delta n/n$, the broadening of the wave spectrum is the dominant effect, and the phenomena of wave-reflection, not observed in this article, could have time to occur even during the linear stage of the instability. Such a regime could thus be favorable to the generation of trapped eigenmodes, at the condition that the density cavities stay stable on a time long enough.

[45] We can conclude that the existence of trapped eigenmodes in the solar wind gives clear indications of the existence of density cavities that are stable on timescales much longer than the time given by a linear theory of ion-sound waves. An important problem to be studied in the future thus consists in the correct description of the time evolution of the density fluctuations, that could be done using the equation of the low-frequency motions where the nonlinearities of the low-frequency density perturbations are sufficiently stronger than those related to the high-frequency waves. Such a study should be done in a forthcoming article.

[46] **Acknowledgments.** The first author is supported by a grant from the Centre National d'Etudes Spatiales.

[47] Philippa Browning thanks Peter Yoon and another reviewer for their assistance in evaluating this paper.

References

Bougeret, J., et al. (2008), S/waves: The radio and plasma wave investigation on the stereo mission, *Space Sci. Rev.*, *136*, 487–528.

Cairns, I. H., and P. A. Robinson (1999), Strong evidence for stochastic growth of langmuir-like waves in earth's foreshock, *Phys. Rev. Lett.*, *82*(15), 3066–3069.

Celnikier, L., C. Harvey, R. Jegou, M. Kemp, and P. Moricet (1983), A determination of the electron fluctuation spectrum in the solar wind using the ISEE propagation experiment, *Astron. Astrophys.*, *126*, 293–298.

Celnikier, L., L. Muschietti, and M. Goldman (1987), Aspects of interplanetary plasma turbulence, *Astron. Astrophys.*, *181*, 138–154.

Chirikov, B. (1979), A universal instability of many-dimensional oscillator systems, *Phys. Rep.*, *52*, 263–379.

Coles, W. A., and J. K. Harmon (1978), Interplanetary scintillation measurements of the electron density power spectrum in the solar wind, *J. Geophys. Res.*, *83*, 1413–1420.

Elskens, Y., and D. Escande (2003), *Microscopic Dynamics of Plasmas and Chaos*, IOP, Bristol, U. K.

Ergun, R. E., et al. (1998), Wind spacecraft observations of solar impulsive electrons events associated with solar type III radio bursts, *Astrophys. J.*, *503*, 535–545.

Ergun, R. E., et al. (2008), Eigenmode structure in solar-wind langmuir waves, *Phys. Rev. Lett.*, *101*, 051101.

Fuchs, V., V. Krapchev, A. Ram, and A. Bers (1985), Diffusion of electrons by coherent wavepackets, *Phys. D*, *14*, 141–160.

Henri, P., C. Braind, A. Mangeney, S. D. Bale, F. Califano, K. Goetz, and M. Kaiser (2009), Evidence for wave coupling in type III emissions, *J. Geophys. Res.*, *114*, A03103, doi:10.1029/2008JA013738.

Kellogg, P. J., K. Goetz, S. J. Monson, S. D. Bale, M. J. Reiner, and M. Maksimovic (2009), Plasma wave measurements with STEREO S/WAVES: Calibration, potential model, and preliminary results, *J. Geophys. Res.*, *114*, A02107, doi:10.1029/2008JA013566.

Krasnoselskikh, V. V., V. V. Lobzin, K. Musatenko, J. Soucek, J. S. Pickett, and I. H. Cairns (2007), Beam-plasma interaction in randomly inhomogeneous plasmas and statistical properties of small-amplitude langmuir waves in the solar wind and electron foreshock, *J. Geophys. Res.*, *112*, A10109, doi:10.1029/2006JA012212.

Matsiborko, N., I. Onishchenko, V. Shapiro, and V. Shevshenko (1972), On nonlinear theory of instability of a mono-energetic electron beam in plasma, *Plasma Phys.*, *14*, 591–600.

Nishikawa, K., and D. Ryutov (1976), Relaxation of relativistic electron beam in a plasma with random density inhomogeneities, *J. Phys. Soc. Jpn.*, *41*, 1757–1765.

O'Neil, T., J. Winfrey, and J. Malmberg (1971), Nonlinear interaction of a small cold beam and a plasma, *Phys. Fluids*, *14*, 1204–1212.

Robinson, P. (1992), Clumpy langmuir waves in type III radio sources, *Sol. Phys.*, *139*, 147–163.

Robinson, P., I. Cairns, and D. Gurnett (1992), Connection between ambient density fluctuations and clumpy langmuir waves in type III radio sources, *Astrophys. J.*, *387*, 101–104.

Sanz-Serna, J. M., and M. P. Calvo (1994), *Numerical Hamiltonian Problems*, Chapman and Hall, London.

Stephenson, G. (1977), Eigen values of the schrodinger equation with a gaussian potential, *J. Phys. A*, *10*, L229.

Sturrock, P. A. (1964), Type III solar radio bursts, in *Proceedings of a Symposium Held at the Goddard Space Flight Center, Greenbelt, Maryland, October 28–30, 1963*, edited by W. N. Hess, p. 357, NASA, Washington, D. C.

Vedenov, A. (1967), Theory of a weakly turbulent plasma, *Rev. Plasma Phys.*, *3*, 229.
Volokitin, A., and C. Krafft (2004), Interaction of suprathermal electron fluxes with lower hybrid waves, *Phys. Plasmas*, *11*, 3165–3176.
Zaitsev, V., N. Mityakov, and V. Rapoport (1972), A dynamic theory of type III solar radio bursts, *Sol. Phys.*, *24*, 444–456.
Zakharov, V. (1972), Collapse of langmuir waves, *Sov. J. Exp. Theor. Phys.*, *35*, 908.
Zaslavsky, A., C. Krafft, and A. Volokitin (2006), Stochastic processes of particle trapping and detrapping by a wave in a magnetized plasma, *Phys. Rev. E, 73*, 016406.

S. D. Bale, SSL, University of California, Berkeley, CA 94720, USA.
V. V. Krasnoselskikh, LPCEE, CNRS, F-45071 Orleans, France.
M. Maksimovic and A. Zaslavsky, Observatoire de Paris, LESIA, F-92195 Meudon, France. (arnaud.zaslavsky@obspm.fr)
A. S. Volokitin, IZMIRAN, 142190 Troistsk, Moscow Region, Russia.